Damage Diagnosis of a Building via Sub-Structural TVARX

C. S. Huang, C. Y. Liu
Dept. of Civil Engineering, National Chiao Tung University, Hsinchu,Taiwan,ROC

W. C. Su
National Center for High Performance Computing, Hsinchu,Taiwan,ROC

SUMMARY:
This paper explores the possibility of using sub-structural instantaneous natural frequencies to locate the storeys of buildings that are damaged in an earthquake event. A damaged storey usually exhibits nonlinear behaviors during a strong enough earthquake, and the corresponding sub-structural natural frequencies often change with time in the earthquake. An appropriate TVARX (time varying autoregressive with exogenous input) model of a sub-structure is established from the sub-structural dynamic responses. The instantaneous natural frequencies of the sub-structure are estimated directly through the identified coefficient matrixes of the TVARX model. The effectiveness of the proposed procedure is verified using numerically simulated earthquake responses of a three-storey shear building and measured responses of a five-storey steel frame under shaking table tests.

Keywords: TVARX, sub-structure approach, instantaneous modal parameters

1. INTRODUCTION

A structure may sustain damage either when subjected to severe loading, such as a strong earthquake, or when its material is degraded. The serviceability and safety of structures rely on the detection and location of structural damage. Early detection of structural degradation can prevent catastrophic failure. Consequently, the development of structural health monitoring systems has received considerable attention over the last two decades. The capability of detecting structural damages and locating damaged areas, based on measured dynamic responses, is of practical importance.

It was mentioned in review articles (Natke, 1988; Mottershead and Friswell, 1993; Salawu, 1997; Farrar *et al*., 2001; Chang *et al*., 2003; Brownjohn, 2007) that vibration-based damage detection methods are simple and widely adopted. Vibration-based damage detection methods typically employ the modal frequencies, damping ratios, and modal shapes of a whole structure. Theoretically, changes in stiffness, damping and mass of a structure should yield changes in its dynamic characteristics. Cawley and Adams (1979), Friswell *et al*. (1994), Hearn and Tesla (1991), Messina *et al*. (1998), and Zapico and González (2003) presented various methods exploiting the modal frequencies of full structures to detect damage. These methods are not so effective as expected because modal frequencies mainly depend on the global behaviors of the structure, whereas damage is a rather local phenomenon. To overcome this difficulty, Su *et al*. (2012) simply applied the sub-structural natural frequencies to locate the possible damaged storeys of a shear building. Some indexes have also been proposed, based on modal shape information. They include such as MAC (Modal Assurance Criterion) (Allemang and Brown, 1983) COMAC (Coordinate Modal Assurance Criterion) (Lieven and Ewins, 1988), MSE (Modal Strain Energy) (Hu *et al*., 2006) and EEQ (Elemental Energy Quotient) (Law *et al*., 1998). MAC and COMAC are easy to obtain, but they are not very sensitive to the existence of damage.

Most of the vibration-based methodologies available in the literature require both the reference data (the data without damage) and the data after damage. The reference data are usually not available or

difficult to obtain because the reference data can be affected by the environments, such as temperature (Moser and Moaveni, 2011). Therefore, it is desirable, without any reference data, to determine whether a building is damaged or not and to locate further the damaged stories from the dynamic responses of the building under a severe event, such as a strong earthquake.

In this work, we present an approach using a TVARX model and a sub-structure technique to identify the instantaneous modal parameters of a full structure and its sub-structures. One can easily judge whether a building is damaged or not and further locate the damaged storeys in an event from the instantaneous natural frequencies obtained from dynamic responses of the building under the event. The TVARX model is established using the methodology proposed by Huang *et al*. (2009), who employed a moving least-squares technique to develop suitable shape functions to expand the coefficient functions in the TVARX model. The sub-structure scheme used in Su *et al*. (2012) is also adopted herein.

2. METHODOLOGY

The time-varying structural system encountered in civil and mechanical engineering can be described by the following equations of motion,

$$\mathbf{M}\ddot{\mathbf{x}} + \mathbf{C}\dot{\mathbf{x}} + \mathbf{K}\mathbf{x} = \mathbf{f}\ , \tag{2.1}$$

where **M**, **C** and **K** are mass, damping and stiffness matrices, respectively, and **C** and **K** are functions of time, while **x** and **f** are displacement and force vectors, respectively. A building may behave nonlinearly when subjected to a large earthquake, and its **C** and **K** are functions of time. Consequently, the instantaneous modal parameters of the building change with time. The damaged storeys of the building can be located from the changes of the instantaneous natural frequencies of sub-structures with time.

The equations of motion in a discrete form are equivalent to

$$\mathbf{y}(t) = \sum_{i=1}^{I} \mathbf{\Phi}_i(t)\mathbf{y}(t-i) + \sum_{j=0}^{J} \mathbf{\Theta}_j(t)\mathbf{f}(t-j) + \mathbf{a}_n(t)\ , \tag{2.2}$$

where $\mathbf{y}(t\text{-}i)$ and $\mathbf{f}(t\text{-}i)$ are the vectors of measured responses and input forces at time $t\text{-}i\,\Delta t$, respectively; $1/\Delta t$ is the sampling rate of the measurement, $\mathbf{\Phi}_i(t)$ and $\mathbf{\Theta}_j(t)$ are matrices of coefficient functions to be determined in the model, and $\mathbf{a}_n(t)$ is a vector representing the residual error accommodating the effects of measurement noise, modeling errors and unmeasured disturbances. Equation (2.2) is known as TVARX model. The measured displacement responses are used for $\mathbf{y}(t\text{-}i)$ to ensure that instantaneous modal parameters can be directly identified from $\mathbf{\Phi}_i(t)$ without a systematic error (Huang *et al*., 2009).

Following the method proposed by Huang *et al*. (2009), each coefficient function in $\mathbf{\Phi}_i(t)$ and $\mathbf{\Theta}_j(t)$ is linearly expanded by the so called shapes functions constructed by a set of basis functions, which are polynomials herein, through a moving least-squares approach (Lancaster and Šalkauskas, 1990). Let $\phi_{kl}^i(t)$ and $\theta_{kl}^i(t)$ denote (k, l) element of $\mathbf{\Phi}_i(t)$ and $\mathbf{\Theta}_j(t)$, respectively, and they are expressed as

$$\phi_{kl}^i(t) = \boldsymbol{\varphi}(t)\overline{\phi}_{kl}^i \quad \text{and} \quad \theta_{kl}^i(t) = \boldsymbol{\varphi}(t)\overline{\vartheta}_{kl}^i \tag{2.3}$$

where $\boldsymbol{\varphi}(t) = \mathbf{p}^T(t)^T \mathbf{A}^{-1}(t)\mathbf{Q}(t)$ is a vector of shape functions,

$\mathbf{A}(t) = \sum_{l=1}^{\bar{l}} W(t,t_l)\mathbf{p}(t_l)\mathbf{p}^T(t_l)$, $\mathbf{Q}(t) = [\mathbf{q}_1,\ \mathbf{q}_2, \ldots,\ \mathbf{q}_{\bar{l}}]$, $\mathbf{q}_l = W(t,t_l)\mathbf{p}(t_l)$, $\mathbf{p}^T = (1,\ t,\ t^2, \ldots, t^{\bar{N}})$,

W is a weight function, $\bar{l}$ is the number of nodal points used for each coefficient function, $\bar{\boldsymbol{\phi}}_{kl}^i$ and $\bar{\boldsymbol{\vartheta}}_{kl}^i$ are two unknown vectors of coefficients for $\phi_{kl}^i(t)$ and $\theta_{kl}^i(t)$, respectively. Many weight functions can be used in the above formulation (Liu, 2003). In this work, the exponential weight function is applied:

$$W(t_m, t_p) = \begin{cases} e^{-((t_m - t_p)/0.3d)^2} & |t_m - t_p|/d \le 1 \\ 0 & |t_m - t_p|/d > 1 \end{cases} \tag{2.4}$$

where d is the support of the weight function.

A least-squares approach is applied to determine $\bar{\boldsymbol{\phi}}_{kl}^i$ and $\bar{\boldsymbol{\vartheta}}_{kl}^i$ by minimizing

$$\bar{E} = \sum_{\bar{n}=1}^{N} (\mathbf{a}_n(t_{\bar{n}}))^T \mathbf{a}_n(t_{\bar{n}}). \tag{2.5}$$

where N is the number of data points to be used in establishing the TVARX model. Then, one can obtain the following equation through typical and lengthy mathematical manipulation

$$\tilde{\boldsymbol{C}} = (\boldsymbol{V}^T\boldsymbol{V})^{-1}\boldsymbol{V}^T\tilde{\boldsymbol{Y}}, \tag{2.6}$$

where $\tilde{\boldsymbol{C}} = \begin{bmatrix} \bar{\boldsymbol{\Phi}}_1 & \bar{\boldsymbol{\Phi}}_2 & \cdots & \bar{\boldsymbol{\Phi}}_I & \bar{\boldsymbol{\Theta}}_0 & \bar{\boldsymbol{\Theta}}_1 & \cdots & \bar{\boldsymbol{\Theta}}_J \end{bmatrix}$, $\tilde{\boldsymbol{Y}} = \begin{bmatrix} \mathbf{y}(t_1) & \mathbf{y}(t_2) & \cdots & \mathbf{y}(t_N) \end{bmatrix}$,

$$V^T = \begin{bmatrix} \boldsymbol{\Gamma}_{1,t_1} & \boldsymbol{\Gamma}_{2,t_1} & \cdots & \boldsymbol{\Gamma}_{I,t_1} & \boldsymbol{\Pi}_{0,t_1} & \boldsymbol{\Pi}_{1,t_1} & \cdots & \boldsymbol{\Pi}_{J,t_1} \\ \boldsymbol{\Gamma}_{1,t_2} & \boldsymbol{\Gamma}_{2,t_2} & \cdots & \boldsymbol{\Gamma}_{I,t_2} & \boldsymbol{\Pi}_{0,t_2} & \boldsymbol{\Pi}_{1,t_2} & \cdots & \boldsymbol{\Pi}_{J,t_2} \\ \vdots & \vdots & \ddots & \vdots & \vdots & \vdots & \ddots & \vdots \\ \boldsymbol{\Gamma}_{1,t_N} & \boldsymbol{\Gamma}_{2,t_N} & \cdots & \boldsymbol{\Gamma}_{I,t_N} & \boldsymbol{\Pi}_{0,t_N} & \boldsymbol{\Pi}_{1,t_N} & \cdots & \boldsymbol{\Pi}_{J,t_N} \end{bmatrix}, \quad \bar{\boldsymbol{\Phi}}_i = \begin{bmatrix} (\bar{\boldsymbol{\phi}}_{11}^i)^T & (\bar{\boldsymbol{\phi}}_{12}^i)^T & \cdots & (\bar{\boldsymbol{\phi}}_{1n}^i)^T \\ (\bar{\boldsymbol{\phi}}_{21}^i)^T & (\bar{\boldsymbol{\phi}}_{22}^i)^T & \cdots & (\bar{\boldsymbol{\phi}}_{2n}^i)^T \\ \vdots & \vdots & \ddots & \vdots \\ (\bar{\boldsymbol{\phi}}_{n1}^i)^T & (\bar{\boldsymbol{\phi}}_{n2}^i)^T & \cdots & (\bar{\boldsymbol{\phi}}_{nn}^i)^T \end{bmatrix},$$

$$\bar{\boldsymbol{\Theta}}_j = \begin{bmatrix} (\bar{\boldsymbol{\vartheta}}_{11}^j)^T & (\bar{\boldsymbol{\vartheta}}_{12}^j)^T & \cdots & (\bar{\boldsymbol{\vartheta}}_{1n'}^j)^T \\ (\bar{\boldsymbol{\vartheta}}_{21}^j)^T & (\bar{\boldsymbol{\vartheta}}_{22}^j)^T & \cdots & (\bar{\boldsymbol{\vartheta}}_{2n'}^j)^T \\ \vdots & \vdots & \ddots & \vdots \\ (\bar{\boldsymbol{\vartheta}}_{n1}^j)^T & (\bar{\boldsymbol{\vartheta}}_{n1}^j)^T & \cdots & (\bar{\boldsymbol{\vartheta}}_{nn'}^j)^T \end{bmatrix}, \quad \boldsymbol{\Gamma}_{i,t} = \mathbf{y}(t-i) \otimes \boldsymbol{\varphi}(t)^{\mathrm{T}}, \quad \boldsymbol{\Pi}_{j,t} = \mathbf{f}(t-j) \otimes \boldsymbol{\varphi}(t)^{\mathrm{T}}, \text{ and}$$

$\otimes$ denotes Kronecker product. After determining $\bar{\boldsymbol{\phi}}_{kl}^i$ and substituting them into Eq. (2.3), one obtains $\boldsymbol{\Phi}_i(t)$. Then, like determining modal parameters from an ARX model, one can obtain the instantaneous modal parameters of the time-varying system from $\boldsymbol{\Phi}_i(t)$ (Huang, 2001).

The assumption of rigid floors is valid for most buildings and three DOFs (two horizontal displacement components and one torsion angle) are needed to describe the horizontal motions of each floor in an earthquake. When a building is symmetrical, the horizontal displacement components and torsion angle of each floor are uncoupled. Consequently, a building behaviors like a shear building when it is subjected to an earthquake along its symmetric plane. Then, the corresponding **M, K** and **C** are, respectively,

$$\mathbf{M} = \mathrm{diag}(\, m_n \; m_{n-1} \cdots m_2 \; m_1 \,), \tag{2.7a}$$

$$\mathbf{K} = \begin{bmatrix} k_n & -k_n & & & & & \\ -k_n & k_n + k_{n-1} & -k_{n-1} & & & 0 & \\ & -k_{n-1} & k_{n-1} + k_{n-2} & -k_{n-2} & & & \\ & & -k_{n-2} & \cdot & \cdot & & \\ & & & \cdot & \cdot & \cdot & \\ & 0 & & & \cdot & k_3 + k_2 & -k_2 \\ & & & & & -k_2 & k_2 + k_1 \end{bmatrix}, \tag{2.7b}$$

$$\mathbf{C} = \begin{bmatrix} c_n & -c_n & & & & & \\ -c_n & c_n + c_{n-1} & -c_{n-1} & & & 0 & \\ & -c_{n-1} & c_{n-1} + c_{n-2} & \cdot & & & \\ & & \cdot & \cdot & \cdot & & \\ & & & \cdot & \cdot & \cdot & \\ & 0 & & & \cdot & c_3 + c_2 & -c_2 \\ & & & & & -c_2 & c_2 + c_1 \end{bmatrix}. \tag{2.7c}$$

These matrices enable a shear building to be easily decomposed into sub-structures that have two or three DOFs. If the jth sub-structure is defined as having j-1 th, $j^{\text{th,}}$ and j+1th DOFs when $j \neq n$ and $j \neq 1$, then the first sub-structure is associated with the first and second DOFs, while the nth sub-structure has the $(n\text{-}1)^{\text{th}}$ and n^{th} DOFs. The following equations in terms of relative acceleration, velocity, and displacement of two floors can be developed,

$$m_n \ddot{x}_n^r + c_n \dot{x}_n^r + k_n x_n^r = f_n - m_n \ddot{x}_{n-1} \quad \text{for} \quad j = n \tag{2.8a}$$

$$m_j \ddot{x}_j^r + c_j \dot{x}_j^r + k_j x_j^r = f_j - m_j \ddot{x}_{j-1} + c_{j+1} \dot{x}_{j+1}^r + k_{j+1} x_{j+1}^r \qquad \text{for } j = 2 \sim (n-1) \tag{2.8b}$$

$$m_1 \ddot{x}_1 + c_1 \dot{x}_1 + k_1 x_1 = f_1 + c_2 \dot{x}_2^r + k_2 x_2^r \quad \text{for } j\text{=1} \tag{2.8c}$$

where $x_j^r = x_j - x_{j-1}$. If an MISO TVARX model with x_j^r as output and f_j, x_{j-1} and x_{j+1}^r as inputs is constructed for each j=2 to (n-1), then the instantaneous natural frequency of the jth sub-structure, which is theoretically $\sqrt{k_j(t)/m_j}$ (Hz), should be determinable. Similarly, we can establish an MISO TVARX model for the first and n^{th} sub-structures.

3. VERIFICATION

Numerically simulated responses of a three-storey shear building were processed to demonstrate the accuracy and effectiveness of the proposed approach in determining instantaneous modal parameters of the building and locating damaged storeys. The mass of each floor of the shear building is $m_1 = 0.2$ ton and $m_2 = m_3 = 0.1$ ton, while the stiffness of each story is $k_1 = 10[1 - 0.2\sin(\pi t/5)]$ kN/m and $k_2 = k_3 = 20$ kN/m. The damping coefficients in the damping matrix $\mathbf{C}$ are $c_1 = 0.15[1 + 0.5\sin(\pi t/5)]$ kN•sec/m and $c_2 = c_3 = 0.1$ kN•sec/m. The material properties of the first story are periodic functions of time.

Figure 1 depicts the time histories of input ground acceleration and displacement responses at each floor. One can establish an appropriate TVARX model from these input and responses by employing the formulation given in the preceding section. The identified instantaneous natural frequencies and modal damping ratios are shown in Fig. 2, which also demonstrates the excellent agreement between

the identified results and the true values. The differences between the identified natural frequencies and the true ones are less than 0.1%, while the identified modal damping ratios differ from the true values by less than 0.3%.

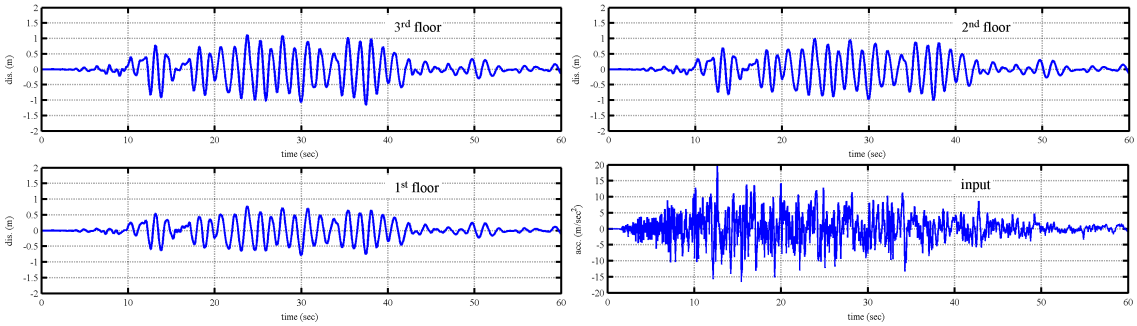

Figure 1. Time histories of simulated responses and input

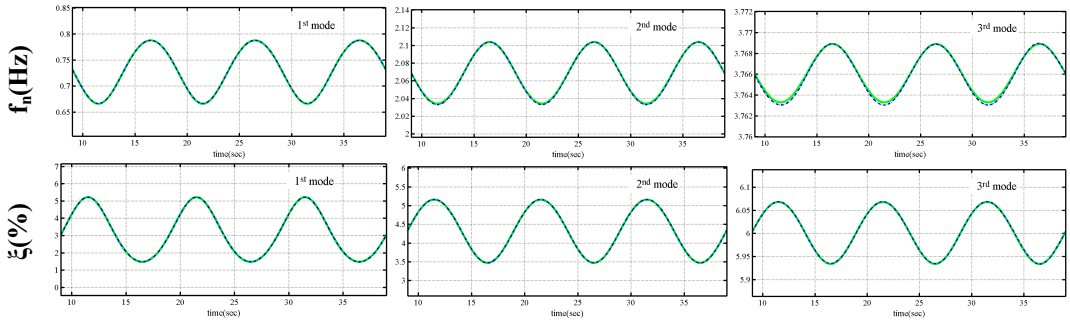

Figure 2. Instantaneous modal parameters identified from responses without noise(true I.D.)

An MISO TVARX model was established for the third sub-structure by using the ground accelerations and displacement responses of the second floor as input and the displacement responses of the third floor as output. The identified instantaneous natural frequencies and damping ratios of the sub-structure are illustrated in Fig. 3 and do not change significantly with time. The differences between the identified frequencies and the true ones are less than 0.01%, while the differences are less than 0.02% for the identified damping ratios. Similarly, an MISO TVARX model was also built up for the first sub-structure. The identified instantaneous natural frequencies and damping ratios of the sub-structure are also depicted in Fig. 3. The differences between the identified results and true ones are less than 0.2%.

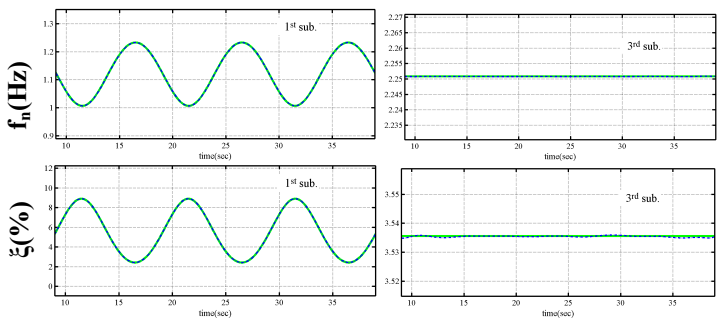

Figure 3. Sub-structural instantaneous modal parameters identified from responses without noise
(true I.D.)

In reality, measured responses always contain noise. To simulate this fact, independent Gaussian white noise with a 5% variance in the noise-to-signal ratio (NSR) was randomly added to the computed displacement responses and input base excitation. Figures 4 and 5, similar to Figs. 2 and 3,

respectively, show the instantaneous natural frequencies and modal damping ratios identified from these noisy data. The agreement between the identified results and the true ones shown in Figs. 4 and 5 is not as good as that in Figs. 2 and 3, respectively. Nevertheless, the accuracy of the identified results is still acceptable. In Figs. 4 and 5 the identified instantaneous natural frequencies are different from the exact values by less than 3%, while the differences between the identified modal damping ratios and the exact values are less than 20%.

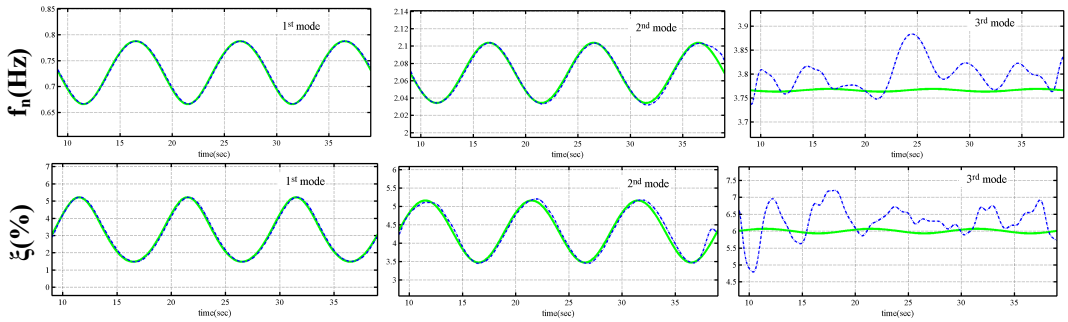

Figure 4. Instantaneous modal parameters identified from noisy responses (NSR=5%)(true I.D.)

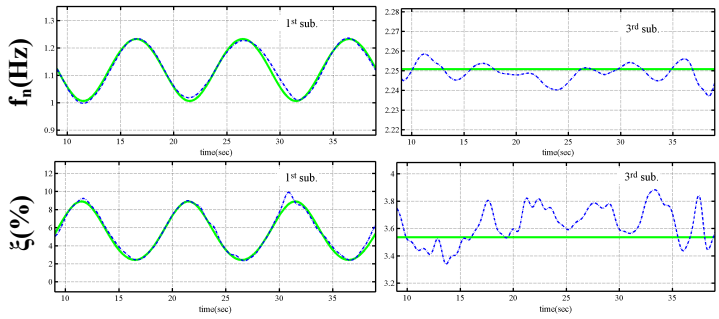

Figure 5. Sub-structural instantaneous modal parameters identified from noisy responses (NSR=5%) (true I.D.)

4. APPLICATION TO SHAKING TABLE TESTS

The measured responses of a five-story symmetric steel frame in shaking table tests (see Fig. 6) were processed to demonstrate the applicability of the present approach to real measured data. The five-story steel frame under consideration was 3m long, 2m wide and 13 m high (see Fig. 6). Lead blocks were piled on each floor, such that the mass of each floor was approximately 3664kg. The frame was subjected to base excitation of the Kobe earthquake with different reduced levels (Yeh *et al.*, 1999). Figure 7 depicts the displacement responses of the first and fifth floors in the long-span direction for the frame, subjected to 60% of the Kobe earthquake. The frame was yielded at the columns of the first storey under such earthquake. The longitudinal strain responses at a yielded column are given in Fig. 8, in which the residual strains are observed.

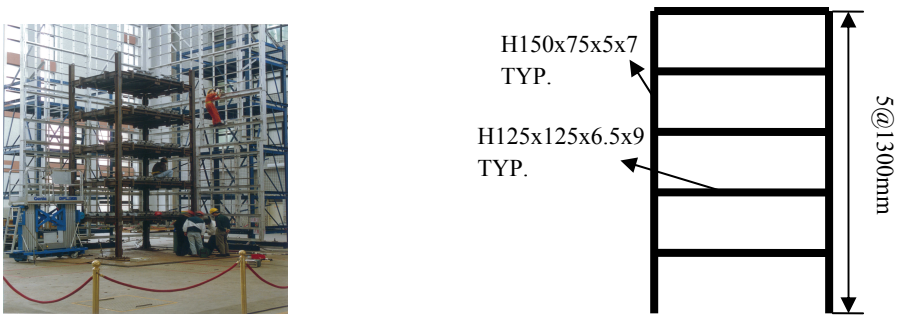

Figure 6. Photo and simple sketch of five-story frame

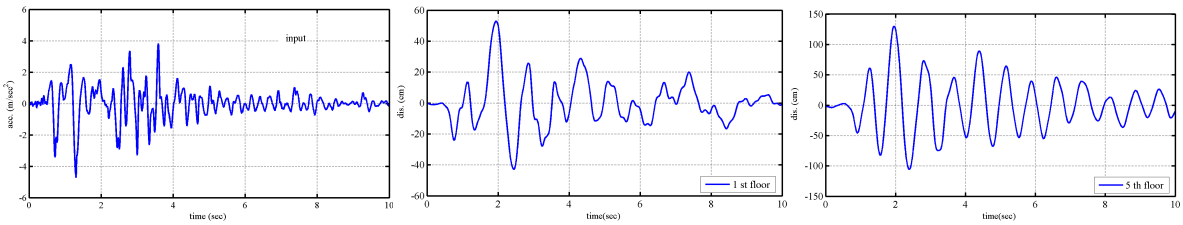

Figure 7. Responses of frame under 60% of the Kobe earthquake

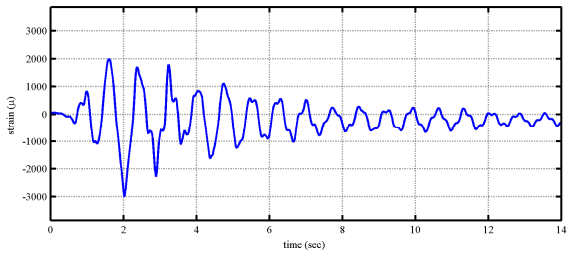

Figure 8. Strain responses at a column

Figures 9 and 10 show the variations of the identified instantaneous natural frequencies and modal damping ratios with time. The results were identified by processing the measured displacement or acceleration responses at all floors, subjected to 10% and 60% of the Kobe earthquake, respectively. Because no nonlinear behaviors were observed when the frame was subjected to 10% of the Kobe earthquake, the natural frequencies and modal damping ratios should be theoretically constants in Fig. 9. Nevertheless, Fig. 9 reveals that the variations of the identified natural frequencies along time are less than 2%, while the variations of the identified damping ratios are much larger.

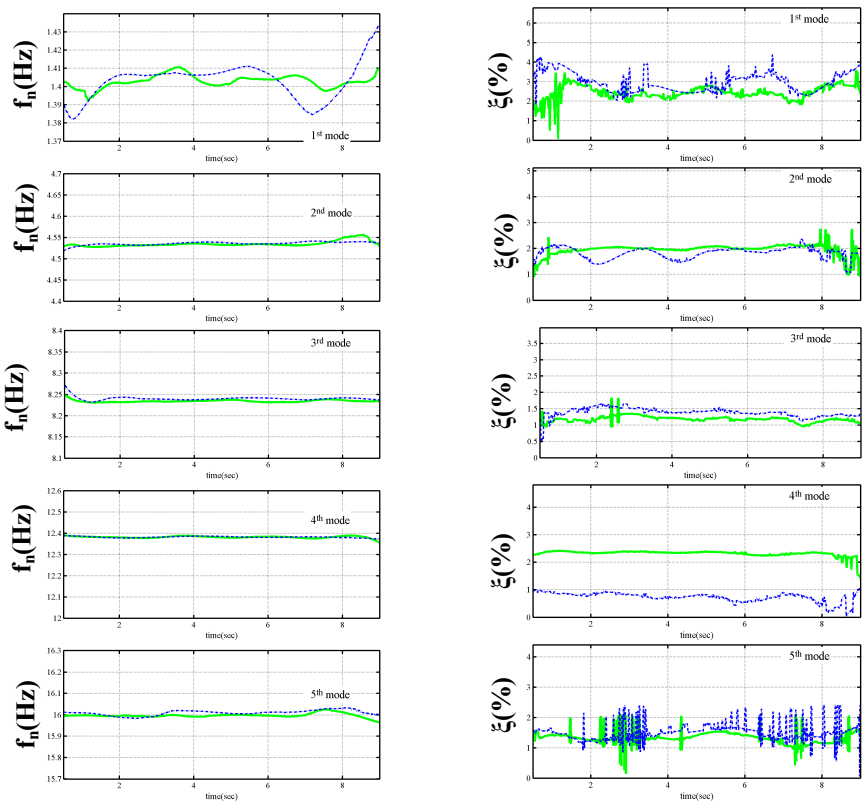

Figure 9. Instantaneous modal parameters identified from the responses under 10% of the Kobe earthquake (dis. acc.)

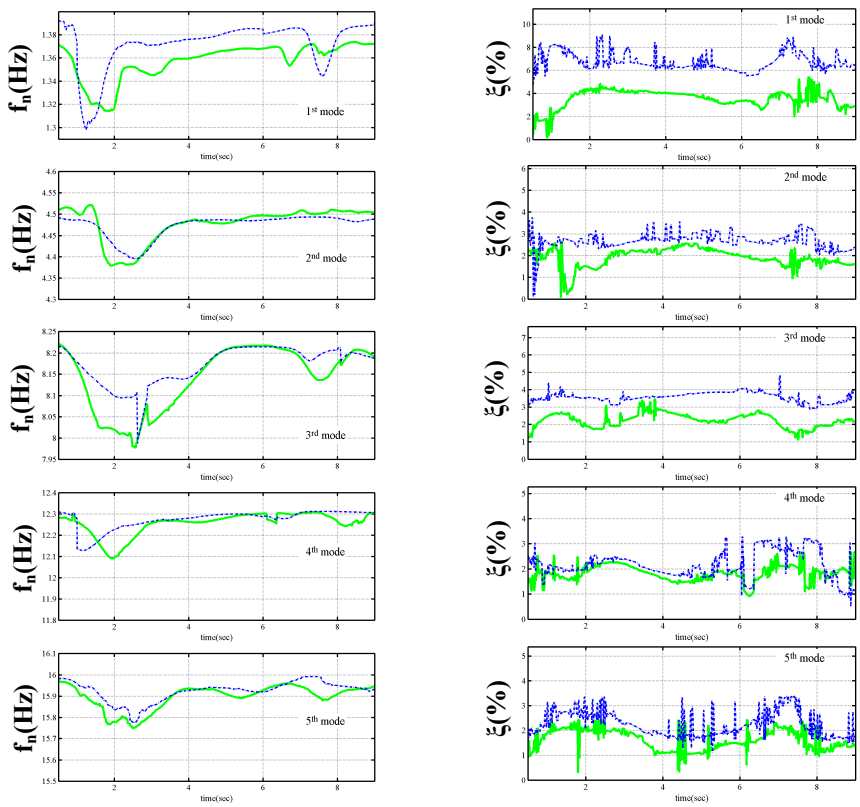

Figure 10. Instantaneous modal parameters identified from the responses under 60% of the Kobe earthquake (dis. acc.)

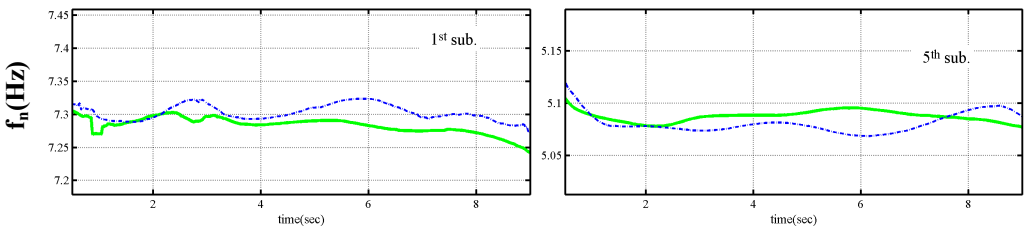

(A) 10% Kobe

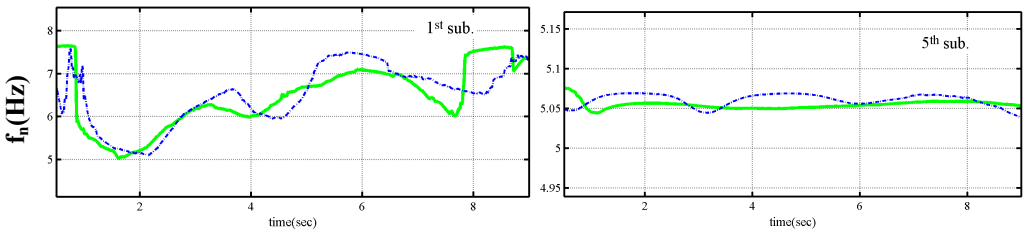

(B) 60% Kobe

Figure 11. Identified instantaneous natural frequencies of sub-structures (dis. acc.)

The frame behaved nonlinearly when it was subjected to 60% of the Kobe earthquake. Figure 10 discloses significant variations of instantaneous natural frequencies with time. The minimum natural frequencies of different modes occur at t=2 sec around, which is about the moment when we begin to observe residual strains in Fig. 8. The maximum reduction of 4.4% in natural frequencies occurs in the first mode.

Figure 11 illustrates the variations of the identified instantaneous natural frequencies of the first and fifth sub-structures. As expected, the instantaneous natural frequencies of the first and fifth storeys do

not significantly change with time when the frame is subjected to 10% of the Kobe earthquake. The variations of natural frequencies with time are less than 1% of the mean values. On the other hand, when the frame is subjected to 60% of the Kobe earthquake, the instantaneous natural frequencies of the first storey significantly change with time, but the instantaneous natural frequencies of the fifth storey do not. The instantaneous natural frequency of the first storey at t=2 sec around is 33% less than the maximum value. This demonstrates the possibility of using the instantaneous natural frequencies of sub-structures to locate the damaged stroeys.

Huang *et al*. (2009) showed that a systematic error occurs in identifying instantaneous natural frequencies and damping ratios if velocity or acceleration responses are employed to construct a TVARX model, and the significance of the error depends on the change rate of stiffness and damping of the structure under consideration. Figures 9-11 reveal that the differences between the instantaneous natural frequencies obtained from the displacement responses and those obtained from the acceleration responses under the 60% of the Kobe earthquake are more significant than those for the 10% of the Kobe earthquake. However, one still can clearly determine whether the frame is damaged or not and locate the damaged storeys from the instantaneous natural frequencies identified by using the acceleration responses.

5. CONCLUDING REMARKS

This work presented a novel approach for locating damaged storeys of a building based on the instantaneous natural frequencies of sub-structures. The instantaneous natural frequencies are accurately determined from the coefficients functions of TVARX models, which are expanded by shape functions constructed through a moving least-squares approach. The main advantages of the present approach are simple and no reference data (such as the data of the building without damage) needed. The proposed approach was demonstrated on a three-storey shear building under earthquake excitation and a five-storey steel frame under shaking table tests. The success of the proposed approach when applied to the experimental responses demonstrates its practical applicability to a real symmetrical building.

ACKNOWLEDGEMENTS
The authors would like to thank the National Science Council of the Republic of China, Taiwan, for financially supporting this research under Contract No. NSC 100-2221-E-009-093-MY2. The appreciation is also extended to the National Center for Research on Earthquake Engineering for providing shaking table test data.

REFERENCES

Allemang, R. J. and Brown, D. L. (1983). A correlation coefficient for modal vector analysis. *Proceedings of the First International Modal Analysis Conference*. 110-116.

Brownjohn, J. M. W. (2007). Structural health monitoring of civil infrastructure. *Philosophical Transactions of the Royal Society A; Mathematical, Physical and Engineering Science* **365:1851**,589-622.

Cawley, P. and Adams, R. D. (1979). The location of defects in structures from measurements of natural frequencies. *Journal of Strain Analysis* **14:2**,49-57.

Chang, P. C., Flatau, A. and Liu, S. C. (2003). Review paper: health monitoring of civil infrastructure. *Structural Health Monitoring, An International Journal* **2:3**,257-267.

Farrar, C. R., Doebling, S. W. and Nix, D. A. (2001). Vibration-based structural damage identification. *Philosophical Transactions of the Royal Society A; Mathematical, Physical and Engineering Science* **359:1778**,131-150.

Friswell, M.I., Penny, J. E. T. and Wilson, D. A. L. (1994). Using vibration data and statistical measures to locate damage in structures. T*he International Journal of Analytical and Experimental Modal Analysis* **9:4**,239-254.

Hearn, G. and Tesla, R. B. (1991). Modal analysis for damage detection in structures. J*ournal of Structural Engineering, ASCE* **117:10**,3042-2063.

Hu, H., Wang, B. T., Lee, C. H. and Su, J. S. (2006). Damage detection of surface cracks in composite laminates using modal analysis and strain energy method. *Composite Structures* **74:4**,399-405.

Huang, C. S. (2001). Structural identification from ambient vibration measurement using the multivariate AR model. *Journal of Sound and Vibration* **241:3**, 337-359.

Huang, C. S., Hung, S. L., Su, W. C. and Wu, C. L. (2009). Identification of time-variant modal parameters using TVARX and low-order polynomial function. *Computer-Aided Civil and Infrastructure Engineering* **24:7**,470-491.

Lancaster, P. and Šalkauskas , K. (1990). *Curve and Surface Fitting- An Introduction*, Academic Press, NY.

Law, S. S., Shi, Z. Y. and Zhang, L. M. (1998). Structural damage detection from incomplete and noisy modal test data. *Journal of Engineering Mechanics, ASCE* **124:10**,1280-1288.

Lieven, N. A. J. and Ewins, D. J. (1988). Spatial correlation of mode shapes, the coordinate modal assurance criterion (COMAC). *Proceedings of the 6th International Modal Analysis Conference*. 690-695.

Liu, G. R. (2003). *Mesh Free Methods- Moving beyond the Finite Element Method*, CRC Press, NY.

Messina, A., Williams, E. J. and Contursi, T. (1998). Structural damage detection by a sensitivity and statistical-based method. *Journal of Sound and Vibration* **216:5**,791-808.

Moser, P. and Moaveni, B. (2011). Environmental Effects on the identified natural frequencies of the Dowling Hall footbridge. *Mechanical System and Signal Processing* **25:7**,2336-2357.

Mottershead, J. E. and Friswell, M. I. (1993). Model updating in structural dynamics. *Journal of Sound and Vibration* **167:2**,347-375.

Natke, H. G. (1988). Updating computational models in the frequency domain based on measured data: a survey. *Probabilistic Engineering Mechanics* **3:1**, 28-35.

Salawu, O. S. (1997). Detection of structural damage through changes in frequency: a review. *Engineering Structures* **19:9**,718-723.

Su, W. C., Huang, C. S., Hung, S. L., Chen, L. J. and Lin, W. J. (2012). Damage diagnosis to a shear building based on its sub-structural natural frequencies. *Engineering Structures* **39**,126-138.

Yeh, S. C., Cheng, C. P. and Loh, C. H. (1999). Shaking table tests on scales down five-storey steel structures. *Rep. No. NCREE-99-002, National Center for Research on Earthquake Engineering,* Taipei, Taiwan (in Chinese)

Zapico, J. L. and González, M. P. (2003). Damage assessment using neural networks. *Mechanical System and Signal Processing* **17:1**,119-125.